Calorimetric Studies of 7000 Series Aluminum Alloys: II. Comparison of 7075, 7050, and RX720 Alloys

PHILIP N. ADLER AND RICHARD DeIASI

Differential scanning calorimetry (DSC) in conjunction with transmission electron microscopy (TEM) are used to characterize the matrix precipitate structure of high strength and overaged tempers of three 7000 series aluminum alloys. Excellent consistency exists between the DSC results, based on the dissolution behavior of existing precipitates, and TEM observations. Comparison is made between matrix precipitate constituency and mechanical properties. A significantly high GP zone particle density was observed in a high strength 7050 alloy temper, but this temper did not have higher strength than other predominantly GP zone matrix tempers. Maximum strength was observed in a 7050 alloy temper that contained approximately equal amounts of GP zones and η' phase precipitates. Strengthening appears to be based on the contribution of both coherent GP zones and semicoherent η' precipitates. Use of the DSC approach and the free energy of activation for precipitate dissolution are recommended as rapid and quantitative means of precipitate identification.

As indicated by the previous paper in this series,[1] differential scanning calorimetry (DSC) provides a rapid and quantitative means of matrix precipitate characterization for 7075 aluminum alloy. The thermodynamic and kinetic parameters associated with dissolution of existing precipitate phases are sensitive means by which the matrix microstructure can be identified. Other 7000 series alloys of the Al-Zn-Mg and Al-Zn-Mg-Cu types are similarly strengthened by matrix precipitate structures consisting of some combination of GP zones, η' and η phases.[2,3] Therefore, the DSC approach should be applicable to characterization of the precipitate structure in these other alloys. In the present work, comparison is made between the matrix microstructure in the high strength and overaged tempers of three 7000 series aluminum alloys, 7075, 7050, and RX720 (the RX720 alloy has also been referred to as BAR). Matrix microstructures are characterized using both DSC and transmission electron microscopy (TEM), with TEM serving to verify the DSC analysis. Mechanical properties were also measured to assist in the comparison of these alloys.

The recent development of 7050 and RX720 aluminum alloys was based on studies of the role of minor addition elements on quench sensitivity.[4-11] By reducing quench sensitivity, thicker sections of uniform strength can be fabricated. It was found that by substitution of Zr for Cr, quench sensitivity could be substantially reduced while the desired recrystallization suppressing effect of Cr was maintained. Both 7050 and RX720 contain Zr in place of the Cr found in 7075 alloy. In addition, 7050 and RX720 contain a lower Fe and Si content than 7075; RX720 contains a higher Zn and lower Cu content than the 7050 alloy. The influence of these compositional differences on both matrix precipitate structure and strength is considered.

PHILIP N. ADLER and RICHARD DeIASI are Head, Metallurgy Branch, and Senior Research Scientist, Solid State Physics Branch, respectively, Materials Laboratory, Research Department, Grumman Aerospace Corporation, Bethpage, NY 11714.

Manuscript submitted June 23, 1976.

EXPERIMENT

Samples of 7050 alloy were taken from a 15.2 cm (6 in.) thick hand forging; RX720 samples were obtained from 7.6 cm (3 in.) thick rolled plate stock; 7075 samples were obtained from 7.6 cm (3 in.) thick rolled bar stock. The composition of these materials, determined by using X-ray fluorescence and emission spectroscopy, is listed in Table I.

The 7075 alloy was received in its high strength, stress relieved, T651 temper. Specimens were overaged to the T7351 temper by heat treating at 175°C for 9 h. The RX720 alloy was received in its high strength, T6 temper. Samples were heat treated for 21 h at 163°C to produce the overaged T7 temper.[12] The 7050 alloy was received in an overaged T7352 temper. To attain the high strength T6 temper, solution heat treatment at 480°C for 2 h followed by duplex aging at 120°C for 4 h and then 168°C for 4 h was used.[13] The specimens given this treatment were water quenched following solution heat treatment. Another group of 7050 alloy specimens were aged for 24 h at 120°C following the water quench to approximate the matrix microstructure of RX720-T6 and 7075-T651 alloys. We designate this temper as T6X.

Calorimetric measurements were made using a DuPont 900 Thermal Analyzer containing a DSC plug-in module. This technique has been described[14] and was previously applied to analysis of 7075 aluminum alloy.[15] Sample discs of 0.56 cm (7/32 in.) diam × 0.127 cm (0.050 in.) thickness were prepared from each of the seven tempers under investigation. A minimum of five samples were tested for each temper. Conditions of testing were identical to those reported earlier.[1] Sample preparation for transmission microscopy has also been described.[1]

The stress-strain behavior of each temper was measured and used to determine the 0.2 pct yield strength, ultimate strength, and elongation. A minimum of four specimens from each temper was tested at a cross-heat speed of 5.1×10^{-2} cm/min (2.0×10^{-2} ipm). The uniaxial loading direction of the specimen was parallel

to the short transverse direction of the bar or forging. Vickers diamond pyramid hardness (DPH, at a 5 kg load) was also used to evaluate these tempers. Impressions were made on surfaces that were polished with 1 μm alumina.

RESULTS

Representative matrix microstructures of each of the seven tempers examined are illustrated in the electron micrographs of Figs. 1–3. The high strength and overaged tempers of 7075 and RX720 are shown in Figs. 1 and 2, respectively; the microstructures of the isothermally aged temper, T6X, the highest strength temper, T6, and the overaged temper of the 7050 alloy are shown in Fig. 3. A summary of the TEM observations is given in Table II. Identification of the precipitate phase is based on size consideration and numerous observations of precipitate morphology in isothermally aged samples of 7075 aluminum alloy.[16] The indicated percentages are based on particle count measurements that were made at different areas in each temper. The T6X temper of 7050 consists almost exclusively of spherical GP zones while the higher strength tempers of 7075 and RX720 also contain a small amount of the semicoherent η' phase. On the other hand, the highest strength temper of 7050 has a matrix consisting of approximately equal amounts of GP zones and η'. The matrix precipitate in the overaged temper of the three alloys consists exclusively of η' and η, but differences in the size and amount of matrix precipitates between alloys are evident.

The matrices of high strength and overaged tempers of 7075 contain many large particles in the 0.1 to 0.2 μm size range, as can be seen in Fig. 1. Particles of this type have been described as Cr-rich $Al_{12}Mg_2Cr$

Table I. Chemical Composition, Wt Pct

Alloy	Zn	Mg	Cu	Zr	Cr	Si	Fe	Ti	Mn	Al
7075	6 1	2.4	1.6	N.D.	0 20	0 11	0.20	0 036	0 04	REM
RX720	7 2	2.4	1.4	0.094	N D	0.07	0.08	0.025	N D	REM
7050	6.2	2.2	2.3	0 086	N D	0.07	0.06	0.029	0 03	REM

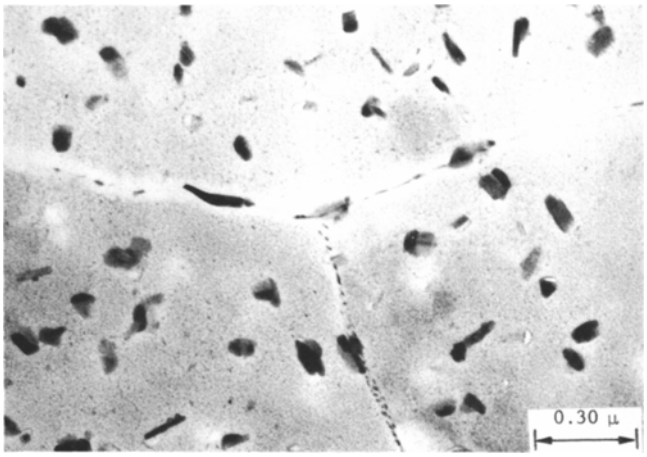

(a)

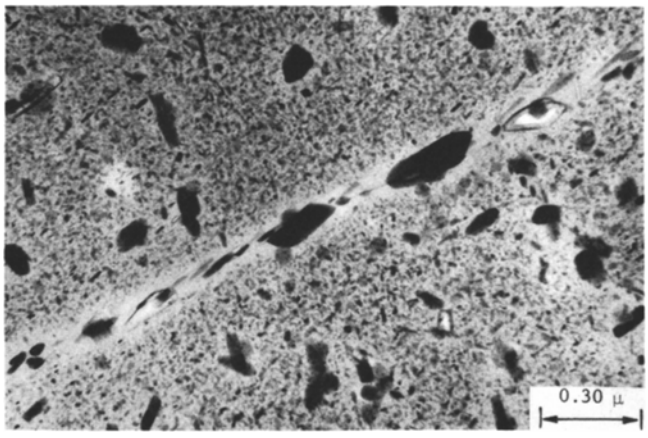

(b)

Fig. 1—Transmission electron micrographs of 7075 aluminum alloy in the (*a*) high strength temper, T651; and (*b*) overaged temper, T7351.

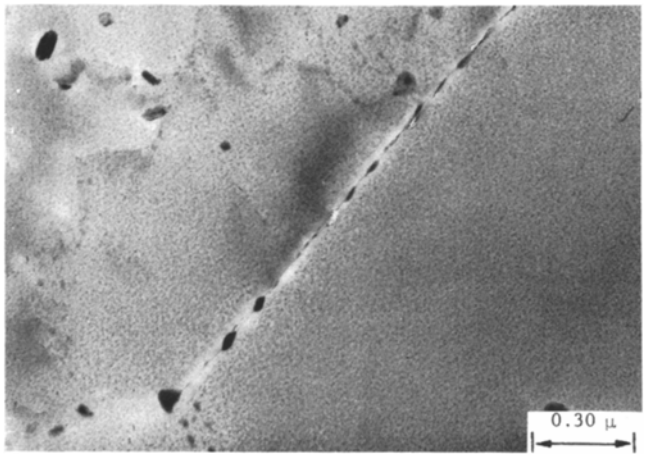

(a)

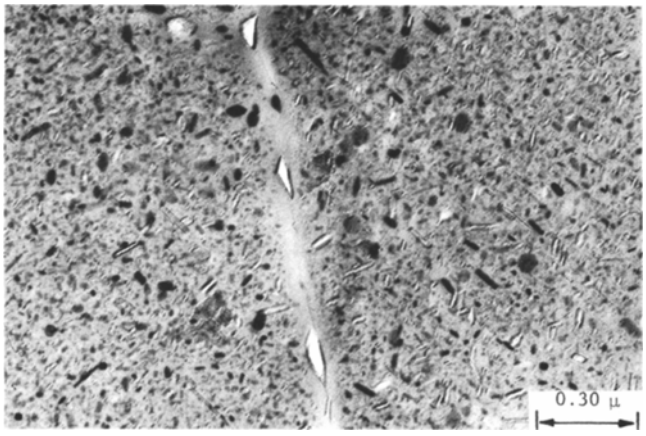

(b)

Fig. 2—Transmission electron micrographs of RX720 aluminum alloy in the (*a*) high strength temper, T6; and (*b*) overaged temper, T7.

Table II. Matrix Precipitate Observed Using Transmission Electron Microscopy

Material	GP Zones	η'	η	Large Particles, μm
7075-T651	~95 pct Spherical	~5 pct (100 to 150Å)	–	(0 1 to 0.2)
RX720-T6	~95 pct Spherical	~5 pct (100 to 150Å)	–	–
7050-T6X	Spherical	–	–	–
7050-T6	~50 pct Spherical	~50 pct (100 to 150Å)	–	–
7075-T7351	–	~65 pct (100 to 150Å)	~35 pct (600Å)	(0 1 to 0 2)
RX720-T7	–	~50 pct (100 to 150Å)	~50 pct (800Å)	–
7050-T7352	–	~90 pct (100 to 150Å)	~10 pct (400Å)	–

phase and Mn-rich $MgZn_2$ phase; these phases do not dissolve during solution heat treatment.[17,18] These particles are only slightly evident in RX720 and almost absent in 7050 (see Figs. 2 and 3). Substitution of Zr for Cr and reduction of the Fe and Si content in RX720 and 7050 alloys appear to have reduced the concentration of these particles. Since previous workers have shown that such particles adversely affect the mechanical properties of 7075,[19,20] their absence in RX720 and 7050 is expected to be beneficial.

The DSC technique was used to characterize the solid state reactions accompanying the dissolution and formation of precipitates for the seven tempers that were examined. Typical results are shown by the differential heat capacity, ΔC_p, *vs* temperature curves in Figs. 4 and 5 for high strength and overaged tempers, respectively. In these illustrations, deviations from the horizontal are indicative of solid state reactions accompanying heating. The basis for computing these curves, as well as their interpretation, is described in the previous paper of this series.[1] In the present work, we will focus on the first endothermic reaction, Region 1, since it describes the existing matrix precipitate, *i.e.*, GP zones and η' phase. The higher temperature endotherm, Region 3, is associated with the dissolution of η phase precipitates. As can be seen in Figs. 4 and 5, the characteristics of Region 1 differ for different alloys of similar temper. Furthermore, the characteristics in Region 1 for the higher strength tempers, Fig. 4, differ from those of the overaged tempers, Fig. 5. The higher strength tempers also undergo an exothermic reaction, Region 2, attributable to the formation and growth of η' and η precipitates.[1] Thermodynamic and kinetic parameters calculated from the behavior in Region 1 enable quantitative comparison between tempers. Values for these parameters are listed in Table III.

The maximum rate of dissolution occurs at the peak dissolution temperature, T_p. For Region 1, T_p is indicative of the relative stability of existing precipitates. As would be expected, the overaged temper of each of the alloys has a higher peak temperature than the higher strength temper. For 7050 alloy, the value of T_p for the highest strength T6 temper is intermediate between that of the predominant GP zone T6X temper and the overaged T7352 temper. Therefore, 7050-T6 contains a matrix precipitate structure that is intermediate in stability, as would be expected for this duplex aged temper.

The area under Region 1 of the ΔC_p *vs* temperature curve is a measure of the heat of reaction associated with precipitate dissolution. This heat, ΔH_R, is proportional to the volume fraction of precipitate and its molar heat of dissolution. Over the higher temperature portion of Region 1, there is also a small exothermic contribution from the reactions associated with the formation and growth of η' and η precipitates. The value of ΔH_R for 7050-T6X is approximately 20 pct higher than for other tempers containing Gp zones. This is consistent with the TEM observations (Figs.

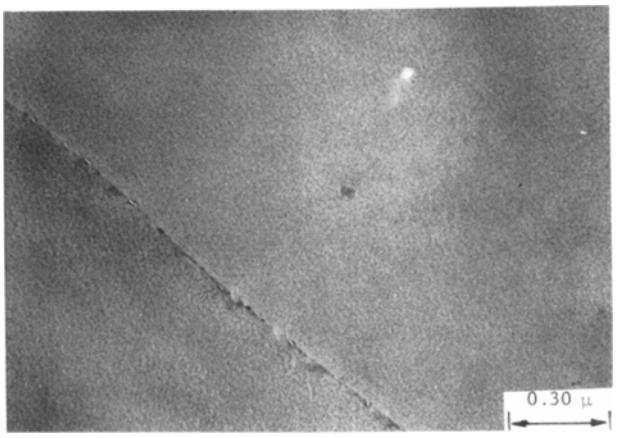

(a)

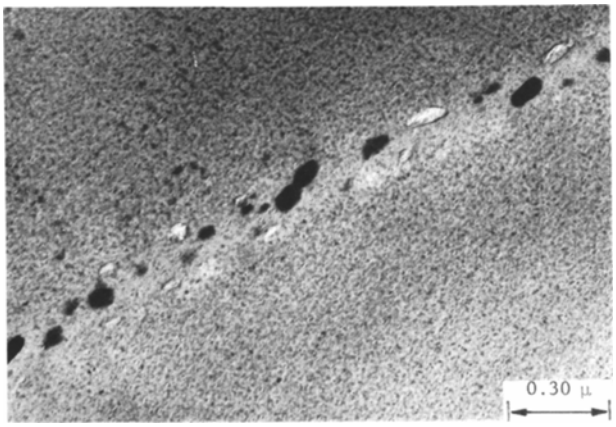

(b)

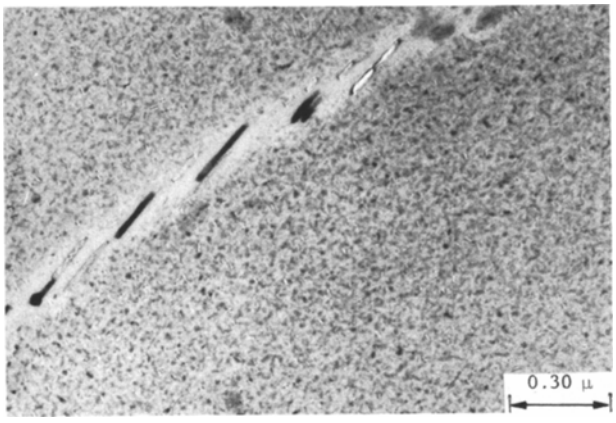

(c)

Fig. 3—Transmission electron micrographs of 7050 aluminum alloy in the (*a*) high strength temper, T6X; (*b*) high strength-duplex aged temper, T6; and (*c*) overaged temper, T7352.

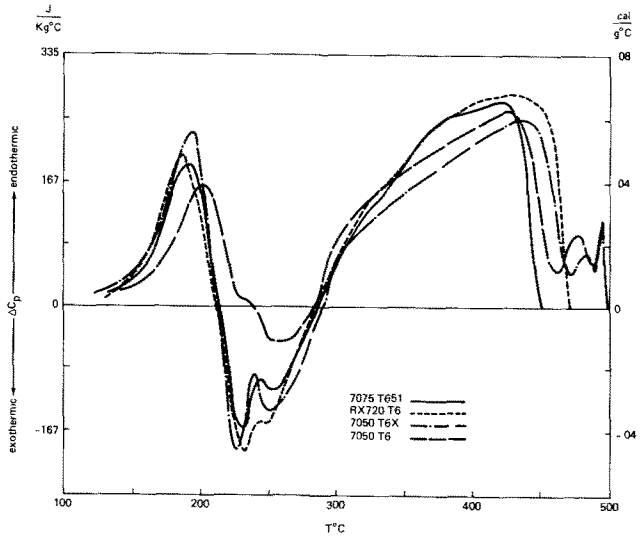

Fig. 4—Differential scanning calorimeter (DSC) results for high strength tempers.

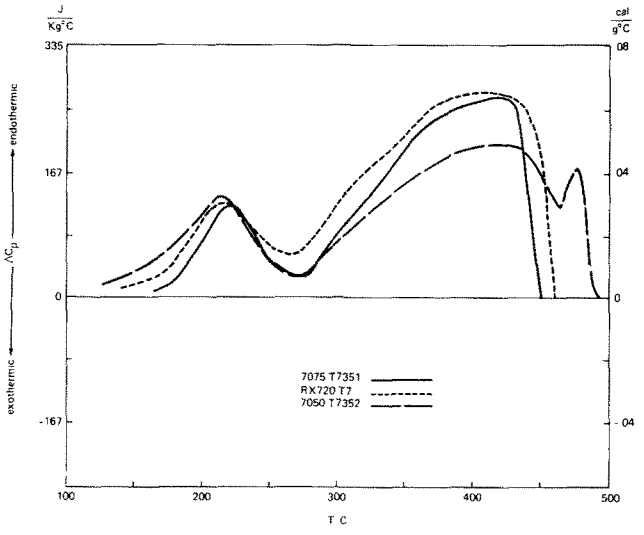

Fig. 5—Differential scanning calorimeter (DSC) results for overaged tempers.

Table III. Dissolution Characteristics* of GP Zones and η' Phase

Material	Peak Temperature, °C (T_p)	Heat of Reaction, ΔH_R		Activation Energy, E_a		Activation Entropy, $\Delta S^\ddagger$		Activation Free Energy, $\Delta G^\ddagger$	
		J/kg	cal/g	kJ/mole	kcal/mole	J/mole–°C	*eu*	kJ/mole	kcal/mole
RX720-T6	184 ± 3	7490 ± 1670	1.79 ± 0.40	111.0 ± 0 8	26.6 ± 0 2	−61 1 ± 0.8	−14 6 ± 0.2	136 ± 1	32 4 ± 0.2
7075-T651	190 ± 2	7370 ± 920	1.76 ± 0.22	108.0 ± 6.7	25 7 ± 1 6	−72 8 ± 15.9	−17.4 ± 3.8	137 ± 10	32.8 ± 2.3
7050-T6X	194 ± 1	9000 ± 170	2.15 ± 0 04	113.0 ± 2.5	27 0 ± 0.6	−61 5 ± 5 9	−14 7 ± 1 4	138 ± 4	32.9 ± 0.9
7050-T6	202 ± 1	7120 ± 290	1.70 ± 0 07	109.0 ± 0 8	26.1 ± 1.0	−76 6 ± 8.4	−18.3 ± 2 0	142 ± 6	33.8 ± 1.4
7050-T7352	213 ± 1	9800 ± 80	2 34 ± 0 02	62 8 ± 0 8	15 0 ± 0.2	−183.0 ± 1 3	−43.6 ± 0.3	147 ± 1	35 2 ± 0 3
RX720-T7	214 ± 1	8120 ± 540	1 94 ± 0.13	85 8 ± 4.2	20 5 ± 1 0	−136.0 ± 8 4	−32.4 ± 2 0	148 ± 6	35 3 ± 1 4
7075-T7351	218 ± 2	6240 ± 630	1.49 ± 0.15	86 2 ± 7.1	20 6 ± 1.7	−136.0 ± 10.0	−32.6 ± 2 4	149 ± 9	35.6 ± 2.1

*One standard deviation indicated

1–3) since 7050-T6X contains the highest GP zone density of all the tempers examined. For the overaged tempers, the values of ΔH_R are not in agreement. This is caused by differences in η' precipitate density and the relative contribution of Region 3 overlap. In any case, the large value of ΔH_R for 7050-T7352, highest of any temper examined, appears to be the result of the high precipitate density of η' in this temper (see Fig. 3(*c*)).

The activation energy, E_a, and activation entropy, $\Delta S^\ddagger$, were also determined from the data in Region 1. For the tempers that contain GP zones, values for both E_a and $\Delta S^\ddagger$ are comparable, ranging from 25.7 to 27.0 kcal/mole for E_a and −14.6 to −18.3 eu for $\Delta S^\ddagger$. Values of E_a as well as $\Delta S^\ddagger$ for overaged RX720 and 7075 tempers are almost equivalent and are quite different from the values for tempers containing GP zones. On the other hand, the overaged 7050-T7352 has the lowest value of E_a and most negative $\Delta S^\ddagger$ of any temper examined.

The relative stability of the precipitate in these tempers should be related to the kinetic barrier for dissolution, *i.e.*, the free energy of activation, $\Delta G^\ddagger$. Values of $\Delta G^\ddagger$ can be calculated from E_a and $\Delta S^\ddagger$ by the following:[20]

$$\Delta G^\ddagger = \Delta H^\ddagger - T\Delta S^\ddagger$$

since

$$E_a = \Delta H^\ddagger + RT$$

$$\Delta G^\ddagger = E_a - T(R + \Delta S^\ddagger)$$

As shown in Table III, values of $\Delta G^\ddagger$ are in total agreement with relative stability based on T_p. Therefore, the extrema in E_a and $\Delta S^\ddagger$ for 7050-T7352, a temper that contains precipitates of intermediate stability by both T_p and $\Delta G^\ddagger$ considerations, suggest unusual characteristics for η' in this material.

Mechanical property results are summarized in Table IV. Tensile specimens were stressed in the short transverse direction, and the results reflect the lower values normally associated with strength in this direction. Direct comparison of the mechanical properties of these alloys should not be made because of their different wrought forms. The 7050-T7352 was fabricated as a 15.2 cm (6 in.) thick hand forging, whereas the other two alloys, RX720-T6 and 7075-T651, were 7.6 cm (3 in.) thick plate and bar stock, respectively. For 7050 aluminum alloy, 7.6 cm (3 in.) plate has been reported to have an approximate 3 Ksi higher longitudinal transverse yield strength than 15.2 cm (6 in.) plate.[13] Therefore, the strengths indicated in Table IV for 7050-T7352 would be expected to be higher for 7.6 cm (3 in.) thick stock. Bearing this thickness

Table IV. Mechanical Properties of Aluminum Alloys*

Alloy	0.2 Pct Yield Strength		Ultimate Strength		Elongation, Pct	D.P Hardness (5 kg Load)
	MPa	Ksi	MPa	Ksi		
7075-T651	458 ± 8	66 4 ± 1.2	529 ± 11	76 7 ± 1.6	3 1 ± 1 2	180 ± 3
RX720-T6	473 ± 19	68 6 ± 2.7	528 ± 20	76 6 ± 2 9	1 6 ± 0 4	200 ± 5
7050-T6X	456 ± 23	66 1 ± 3.3	528 ± 25	76.6 ± 3 6	6 7 ± 3 1	182 ± 2
7050-T6	506 ± 15	73.4 ± 2.1	542 ± 16	78.6 ± 2 3	4.7 ± 2 6	198 ± 5
7075-T7351	386 ± 17	56 0 ± 2.4	455 ± 18	66.0 ± 2.6	3 7 ± 1 4	162 ± 4
RX720-T7	400 ± 8	58.0 ± 1 2	456 ± 15	66.2 ± 2.1	3.4 ± 0.4	171 ± 3
7050-T7352	428 ± 12	62 0 ± 1.7	486 ± 11	70 5 ± 1 6	3.1 ± 0 9	177 ± 6

*Tensile properties measured in the short transverse direction

factor in mind, it is apparent that the overaged 7050-T7352 temper has significantly higher strength than overaged RX720 or 7075 and is almost comparable to high strength 7075-T651 and RX720-T6. Another observation that can be made from the results shown in Table IV is that 7050-T6, which contains approximately equal amounts of GP zones and η' phase, has higher yield and ultimate strengths than the tempers that contain a predominant GP zone matrix microstructure, *i.e.*, 7075-T651, RX720-T6, and 7050-T6X.

DISCUSSION

In the present work, there is excellent agreement between the DSC results and TEM observations. High strength tempers that were observed to contain GP zones in TEM, *i.e.*, 7075-T651, RX720-T6, 7050-T6X, and 7050-T6, exhibit comparable dissolution behavior. They have peak dissolution temperatures, T_p, that are lower than those of overaged tempers; they have similar values of dissolution kinetics for E_a and $\Delta S^{\ddagger}$ that are different than those of overaged tempers; and they undergo an exothermic reaction, Region 2, that is absent in overaged tempers. The high strength tempers also have comparable values of ΔH_R, with the exception of 7050-T6X. The high value of ΔH_R for 7050-T6X is in accord with its high GP zone particle density observed by TEM. For the overaged tempers that were observed to contain $\eta' + \eta$ in their matrix, there is a disparity in the ΔH_R results. For 7050-T7352, the maximum value for ΔH_R can be explained by the high particle density of η' observed in this temper.

While there is general agreement between DSC and TEM results, the sensitivity of DSC reveals differences that exist between tempers of similar microstructural constituency. For example, two of the overaged tempers, 7075-T7351 and RX720-T7, have almost identical values of E_a and $\Delta S^{\ddagger}$ for their dissolution kinetics whereas values of Ea and $\Delta S^{\ddagger}$ for 7050-T7352 are quite different from those of any temper examined. The minimum and maximum values of E_a and $\Delta S^{\ddagger}$, respectively, for 7050-T7352 appear reliable since they lead to a $\Delta G^{\ddagger}$ value of 35.2 kcal/mole, which is in accord with the relative stability of the precipitate in this temper. The significance of the DSC behavior in relation to mechanical strength will now be considered.

In earlier calorimetric study of tempers of 7075 that contained a predominant GP zone matrix, it was concluded that the heat of reaction for matrix precipitate dissolution, ΔH_R, was a measure of GP zone particle number density.[15] This was based on hardness results which had a linear increase with increasing ΔH_R, an assumed GP zone strengthening mechanism, as well as limited TEM observations. In the present work, the DSC and mechanical property results for 7075-T651 and RX720-T6 are consistent with this interpretation. However, the 7050-T6X temper, which essentially contains only GP zones in its matrix, has a 35 pct higher value of ΔH_R than the other two tempers but does not have higher strength. It is apparent that either the enhanced GP zone particle density of 7050-T6X is not affecting strength or the ΔH_R value for this reaction, while indicating an increased volume fraction of GP zones, is not a measure of GP zone particle density. As discussed earlier, TEM observations indicate that 7050-T6X does contain a higher GP zone particle density than the other two high strength tempers. It is likely that the higher Cu content of the 7050 alloy (2.3 pct as compared to 1.4 and 1.6 pct for RX720 and 7075, respectively) contributes to the higher GP zone density of 7075-T6X. Thompson found that Cu acts to nucleate and stabilize the early stages of GP zone formation in Al:5Zn:3Mg.[22] In view of the observed high GP zone density and the high value of ΔH_R for 7050-T6X, it can be concluded that the enhanced GP zone particle density is not contributing to the strengthening relationship observed at lower particle densities. Therefore, there appears to be a maximum strengthening effect attainable in 7000 series aluminum alloys via a GP zone mechanism, and the GP zone particle density in 7050-T6X is in excess of this maximum.

Maximum strength in 7075 aluminum alloy has been reported to correspond to a microstructure that contained a predominant GP zone matrix.[15,16] Similar observations have been made in other Al-Zn-Mg type alloys,[23-25] and Staley has reported that the peak strength in 7050 is developed in a GP zone matrix.[26] Based on these reports, strengthening can be considered to be dependent on the presence and particle density of coherent GP zones. On the other hand, Thomas and Nutting reported that maximum hardness occurred for a microstructure that contained a maximum number of GP zones and η' plates.[27] In reviewing the Thomas and Nutting work, Kelly and Nicholson observed that the microstructure at peak hardness contained a preponderance of η'.[3] Earlier, Nicholson, Thomas, and Nutting had related age hardening in Al-Zn-Mg alloys to a dispersion hardening mechanism caused by η' particles.[28] Others have reported that maximum strength

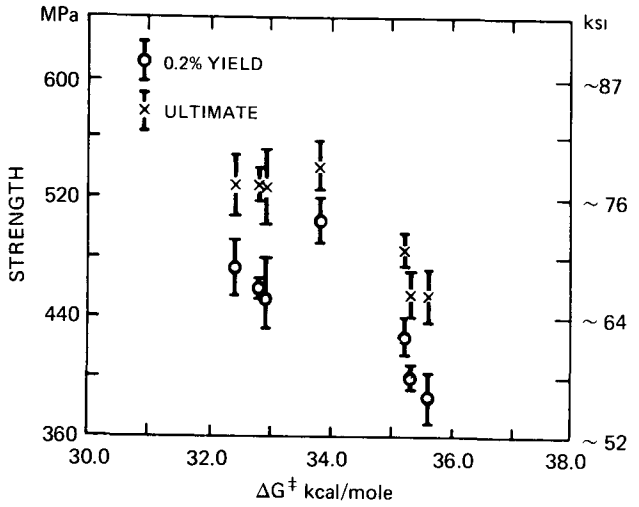

Fig. 6—Mechanical properties as a function of matrix precipitate stability.

occurs when GP zones disappear and η first appears.[2] For the present work, the temper of highest strength, 7050-T6, contains an approximately equivalent concentration of GP zones and η' phase. In addition, the combination does not appear to be one of maximum particle density. The DSC results confirm that the precipitate phases in this temper are intermediate in stability between those of predominantly GP zones and η' phase. This is illustrated in Fig. 6 where the relationship between strength and precipitate stability, $\Delta G\ddagger$, is shown. Maximum strength can be seen to coincide with intermediate precipitate stability, and this is most evident for the yield strength. When GP zones are not present, as is the case for the three overaged tempers, strength is reduced. The high strength exhibited by the 7050-T6 material is likely the result of a combined strengthening effect provided by coherent GP zones and semicoherent η' particles. A more systematic evaluation of the significance of matrix microstructure to strength that investigates the region of intermediate stability using isothermal aging sequences is the subject of an ongoing study that is planned for subsequent publication.

CONCLUSIONS

1) Excellent consistency exists between DSC and TEM analysis for the characterization of matrix precipitates in the three alloys studied.

2) High strength tempers exhibit similar matrix precipitate dissolution behavior, but differences exist that are indicative of differences in stability and particle number density.

3) The dissolution behavior of overaged tempers of 7075 and RX720 are almost identical, but the overaged 7050 contains a large concentration of η' precipitates that have unique dissolution characteristics.

4) There appears to be a saturation in the strengthening effect associated with GP zones.

5) Highest strength was observed for a matrix containing a combination of coherent GP zones and semicoherent η' particles.

6) Use of over-all matrix precipitate stability, described by the free energy of activation for dissolution, is suggested as a quantitative means of precipitate identification to relate to strength.

ACKNOWLEDGMENTS

This work was partially supported by National Aeronautics and Space Administration Contract No. NAS 8-28986. We thank Dr. G. Geschwind for informative discussions and review of this work. Mr. W. Poit assisted in the DSC measurements. We also thank Dr. D. S. Thompson for supplying the RX720 aluminum alloy.

REFERENCES

1. R. Delasi and P N. Adler *Met Trans A*, 1977, vol. 8A, p 1177
2. L F. Mondolfo *Metals Mater*, 1971, vol 5, p 95.
3. A. Kelly and R B. Nicholson *Progr Mater Sci.*, 1963, vol 10, no 3, p. 216.
4. A J Bryant *J. Inst. Metals*, 1966, vol. 94, p 94.
5. Y Baba: *Trans Jap Inst. Metals*, 1968, vol 9, p. 507
6. E DiRusso Report No 16269 ISML (Experimental Inst. of Light Metals), Navara, July 1966
7. M Conserva, E DiRusso, and I Calomi *Met Trans.*, 1971, vol 2, p 1227.
8. D S Thompson, B S. Subramanya, and S A Levy *Met Trans*, 1971, vol. 2, p. 1149
9. H. Y Hunsicker, J T Staley, and R H. Brown *Met. Trans.*, 1972, vol. 3, p. 201.
10. M Conserva and P Fiorini *Met. Trans.*, 1973, vol. 4, p. 857
11. W F Smith and N J. Grant *Met. Trans.*, 1971, vol. 2, p. 1333
12. D. S Thompson· AFML-TR-73-18, April 1973.
13. J T. Staley, H. Y. Hunsicker, and R. Schmidt. *New Aluminum Alloy 7050*, TMS paper selection, 1971.
14. R A Baxter in *Thermal Analysis*, vol 1, p. 65, Academic Press, New York, 1969.
15. P Adler, G Geschwind, and R. Delasi in *Proc of Third International Conference on Thermal Analysis*, 1972, vol 2, p 747, Berkhauser Verlag, Basel, Switzerland.
16. P. N. Adler, R Delasi, and G. Geschwind *Met Trans*, 1972, vol 3, p 3191
17. M S Hunter NASA Report CR-61562, Alcoa Research Laboratories, 1967.
18. M. O Speidel in *International Conference on Fundamental Aspects of Stress Corrosion Cracking*, 1969, p 561, NACE, Houston, Texas
19. S N Singh and M C Flemings *Trans TMS-AIME*, 1969, vol. 245, p 1803.
20. J H. Mulherin and H Rosenthal· *Met Trans*, 1971, vol. 2, p. 427
21. F Daniels and R. A Alberty *Physical Chemistry*, 2nd ed., p. 650, John Wiley and Sons, Inc., New York, N Y, 1962.
22. D S Thompson· in *Thermal Analysis*, vol. 2, p. 1147, Academic Press, New York, N Y, 1969.
23. D. O. Sprowls and R H. Brown· in *International Conference on Fundamental Aspects of Stress Corrosion Cracking*, 1969, p. 466, NACE, Houston, Texas.
24. H Y Hunsicker *Aluminum*, 1967, vol 1, p. 125, ASM, Metals Park, Ohio.
25. W. F. Smith and N. J Grant *Met. Trans.*, 1970, vol 1, p. 979.
26. J T. Staley *Met. Trans.*, 1974, vol 5, p 929.
27. G Thomas and J Nutting *J Inst. Metals*, 1959-1960, vol 88, p. 81.
28. R B Nicholson, G Thomas, and J. Nutting *J Inst. Metals*, 1958-1959, vol. 87, p 429